2019 IEEE/RSJ International Conference on Intelligent Robots and Systems (IROS)
Macau, China, November 4-8, 2019

Development of a Steel Bridge Climbing Robot

Son Thanh Nguyen, Hung Manh La, *IEEE Senior Member*

***Abstract*— Motivated by a high demand for automated inspection of civil infrastructure, this work presents an efficient design and development of a tank-like robot for structural health monitoring. Unlike most existing magnetic wheeled mobile robot designs, which may be suitable for climbing on flat steel surface, our proposed tank-like robot design uses reciprocating mechanism and roller-chains to make it capable of climbing on different structural shapes (e.g., cylinder, cube) with coated or non-coated steel surfaces. The developed robot is able to pass through the joints and transition from one surface to the other (e.g., from flat to curving surfaces). Taking into account several strict considerations (including tight dimension, efficient adhesion and climbing flexibility) to adapt with various shapes of steel structures, a prototype tank-like robot integrating multiple sensors (hall-effects, sonars, inertial measurement unit, Eddy current and cameras), has been developed. Rigorous analysis of robot kinematics, adhesion force, sliding failure and turn-over failure has been conducted to demonstrate the stability of the proposed design. Mechanical and magnetic force analysis together with sliding/turn-over failure investigation can serve as an useful framework for designing various steel climbing robots in the future. The robot is integrated with cameras and Eddy current sensor for visual and in-depth fatigue crack inspection of steel structures. Experimental results and field deployments confirm the adhesion, climbing, inspection capability of the developed robot.**

I. Introduction

The need for automated inspection of civil infrastructures is growing since the current inspection practice is mainly manual and can not meet the demand for frequent and adequate inspection and maintenance [1], [2]. Civil infrastructures like bridges in general or steel bridges in particular are performed by inspectors with visual inspection or using chain dragging for crack and delamination detection, which are very time consuming and not efficient. Often, it is dangerous for the inspectors to climb up and hang on cables to inspect high structures of bridges [3]. Additionally, some areas of the structures are hard to reach or may not be accessible due to their confined space. For example, the Golden Gate bridge, a landmark of the Bay area in San Francisco, California, is manually inspected by a team of 12 rope certified bridge engineers, who have to climb and hang on the high steel structures to perform inspection and evaluation as shown in Fig. 1.

Fig. 1: Current practice of steel bridge inspection: rope certified bridge engineers inspecting the Golden Gate bridge, San Francisco, California [3], source: NBC April 2018.

As an effort to automate the inspection process, there has been some implementations of climbing robots for inspection [4]–[7]. A roller chain, integrated permanent magnets robot was reported in [8]. A legged robot that can transition across structure members for steel bridge inspection was developed [9]. The robot uses permanent magnets integrated with each foot to allow it to hang from a steel bar. In another case, a magnetic wheeled robot, which can carry magneto resistive sensor array for detecting corrosion and cracks, was developed [10]. Similarly, several climbing permanent magnet-robots [11]–[17] were designed to carry non-destructive evaluation (NDE) devices to detect corrosion, weld defects and cracks, and these robots can be applied for inspecting steel structures and bridges. Additionally, significant development of climbing robots for steel structure and bridge inspection has been reported in [18]–[28]. Last, but not least, a surface adapting tank-like robot carrying untouched permanent magnets was developed by Inuktun company for steel structure inspection using camera for visual observation [29].

In summary, most existing designs are developed for particular application with limited functions. Some provide visual inspection only, and some use untouched magnets, which cause the robot much heavier. Most existing designs have fixed distance between the magnet and surface, thus may not work on different types of surface contours. They might be difficult to apply on complicated structures of real bridges that require adaptable, light and effectively data collected robot.

This paper presents a practical climbing robotic system

This work is supported by the U.S. National Science Foundation (NSF) under grants NSF-CAREER: 1846513 and NSF-PFI-TT: 1919127, and the U.S. Department of Transportation, Office of the Assistant Secretary for Research and Technology (USDOT/OST-R) under Grant No. 69A3551747126 through INSPIRE University Transportation Center.The views, opinions, findings and conclusions reflected in this publication are solely those of the authors and do not represent the official policy or position of the NSF and USDOT/OST-R.

The authors are with the Advanced Robotics and Automation (ARA) Lab, Department of Computer Science and Engineering, University of Nevada, Reno, NV 89557, USA. Corresponding author: Hung La, email: hla@unr.edu.

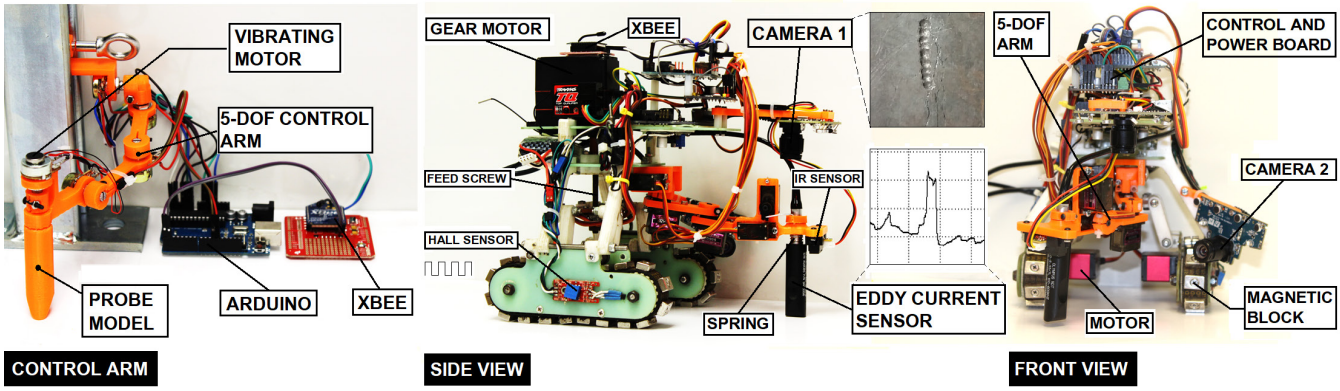

Fig. 2: Steel climbing robotic system. (Left) a simulated robotic arm on the ground station for remote control. (Middle) the side view of the robot. (Right) the front view of the robot. The robot equipped with both camera and Eddy current sensor for visual and non-destructive evaluation of the steel structure.

to provide an efficient solution for steel bridge inspection. The robot can adapt a wide range of different sorts of bridge surfaces (flat, curving, rough) and carry sufficient measurement devices including cameras and Eddy current sensor. The proposed small tank-like robot with reciprocating mechanism features various deformable 3D configurations, which can allow it to transition among steel structure members for efficient inspection. The robot utilizing adhesion force generated by permanent magnets is able to well adhere on steel structures while moving. The roller-chain design allows the robot to overcome obstacles including nuts, bolts, convex and concave corners. To demonstrate the robot's working principle, it has been deployed for climbing on more than 20 steel bridges. Video of this deployment can be seen in the ARA lab website: `https://ara.cse.unr.edu/?page_id=11` or youtube link: `https://www.youtube.com/watch?time_continue=41&v=1Wl9Trd3EoM`

II. Overall Design

The overall design concept of the climbing robot is shown in Fig. 2. The roller-chains embedded with permanent magnets for adhesion force creation enable the robot to adhere to steel surfaces without consuming any power. The control architecture of the robot consists of low-level and high-level controllers. The low-level controller handles tasks including (i) converting velocity and heading command from the high-level controller to Pulse Width Modulation (PWM) data to drive motors, and (ii) reading data from multiple sensors for navigation purposes. The high-level controller is embedded in an onboard computer to enable data processing and ground station communication. Both controllers fuse sensor data to provide desired linear velocity and heading for the robot and acquire data from advanced sensors. Furthermore, the high-level controller sends data wirelessly to ground station for processing and logging.

The robot is equipped with various sensors for navigation as well as steel structure evaluation. There are two video cameras: one for capturing images of inspected surfaces, and the other one for guiding navigation of the robotic arm. There are two 5-DOF robotic arms: one on the robot for navigating the Eddy current sensor probe, and the other one for the operator, who can observe the camera's visual feedback then control this arm for manual operation purposes. For autonomous mode, the arm on the robot uses a mini vibration motor to support it to navigate the Eddy current probe on the steel surface. The robot has two roller-chains, and each roller-chain is integrated with two hall-effect sensors, which are mounted next to each other and close to robot's roller. Since the magnet block inside each roller-chain will move when the robot moves, we can extract the velocity and traveling distance of each roller-chain after combining the data from these two hall-effect sensors. Additionally, an Inertial Measurement Unit (IMU) is used for the robot's localization [30], [31]. Moreover, to avoid falling off, the robot has sonar sensors mounted at the front of the robot to detect if a surface underneath exists.

Fig. 3: (Left) Industrial Eddy current sensor Nortec 600; (Right) sensor probe for data collection.

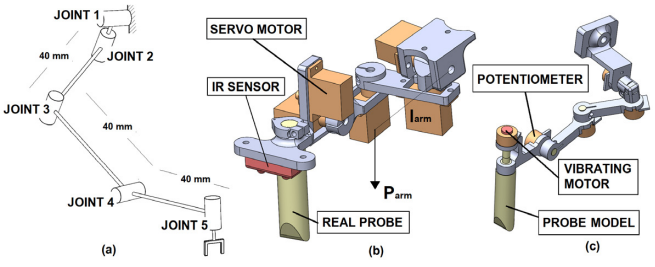

Fig. 4: a) kinematic structure of 5-DOF arm; b) executive arm integrating on the robot; c) controlling arm for user operation in manual mode.

For fatigue crack detection on steel structure, the Eddy current sensor's probe (Nortec 600) as shown in Fig. 3 is integrated with the robot. A mini 5-DOF robotic arm (Fig.

4a) is designed to hold and move the probe for data collection as demonstrated in Fig. 4b.

Maximum moment on joint 1 in Fig. 4b is described as

$$M_{arm} = P_{arm} * l_{arm}, \quad (1)$$

where $P_{arm} = 0.3kg, l_{arm} = 6cm$, so $M_{arm} = 0.18N.m$ Five motors used are 0.25 $N.m$-torque-mini servos, which satisfy (1).

On ground station, the operator observes visual feedback from the camera and then controls a simulated arm (same scale as the one integrated with the robot) by holding and moving a probe model. The moving control signal is wirelessly sent via Xbee module to control the arm on the robot. Five joint's angles are obtained by potentiometers then processed before sending required control angles to servo motors. An IR sensor is mounted on the Eddy current sensor's probe to determine whether the probe approaches the steel surface or not. When distance from IR sensor to the surface meets a calibrated number (45mm), a signal will be sent back to ground station to trigger a tiny vibrating motor on the simulated arm to enable Eddy data collection. Furthermore, a pressure spring is placed between the probe and robotic arm to improve sensor's approaching. This design helps the sensor's probe to efficiently collect Eddy data on complex surfaces such as weld, rough or curving.

III. Mechanical Design and Analysis

A tank-like robot mechanism design is proposed to take advantage of the flexibility in maneuvering. Two motors are used to drive two roller-chains, and another motor is used to drive the transformation of the robot to approach different contour surfaces. The robot's parameters are shown in Table I while the motor's parameters are listed in Table II.

TABLE I: Robot Parameters.

Length	163 mm
Width	145 mm
Height	198 mm
Weight	3 kg
Drive	2 motorized roller-chains and 1 motorized transformation

TABLE II: Motor Parameters.

	Moving motors	**Tranforming motor**
Torque	1.2 N.m (2S Li-Po)	3.2 N.m
Speed	0.12 sec/ 60° (2S Li-Po)	0.15 sec/ 60° (2S Li-Po)
Length	40.13 mm	60.5 mm
Width	20.83 mm	30.4 mm
Height	39.62 mm	45.6 mm
Weight	71 g	156 g
Voltage	6-8.5V (2S Li-Po battery)	6-8.5V (2S Li-Po battery)

A roller-chain is designed to carry 22 Neodymium magnet blocks with poles on flat ends as shown in Fig. 2-front view. With each motion, there will be maximum of 8 magnet blocks contacting the flat steel surface. Roller-chains are designed to enable the robot to overcome several real climbing scenarios including transitioning among surfaces with different inclination levels ($0-90^{\circ}$ change in orientation) or getting rid of being stuck. A reciprocating mechanism has been added in order to transform the robot to adapt with different contour surfaces and specifications of the robot's design is shown in Fig. 5.

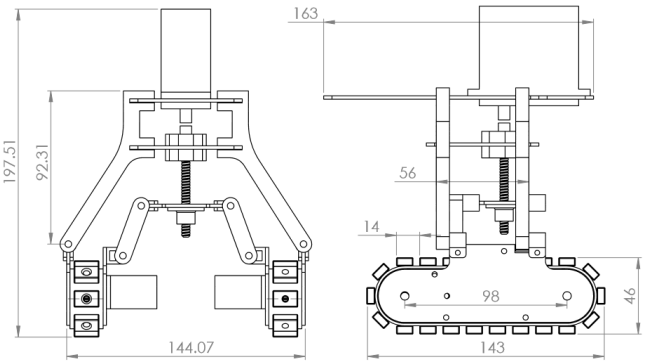

Fig. 5: Reciprocating mechanism for robot transformation and specifications of the robot's design (unit in mm).

We have the magnetic force created by each robot's roller-chain as: $\sum F_{m_j}(j = 1:8)$. Since the robot has two roller-chains, the total magnetic adhesion force, F_m, is:

$$F_m = 2 * \sum F_{m_j}(j = 1:8). \quad (2)$$

A. Robot transformation kinematics

Kinematics analysis of reciprocating mechanism is to calculate radius of steel cylinder (x), that robot can climb on. The feed screw mechanism has gear ratio is $1:19$ with screw pitch is $0.8mm$. Fig. 6 represents kinematics of the robot, and Fig. 7 illustrates a general architecture of the robot's reciprocating mechanism.

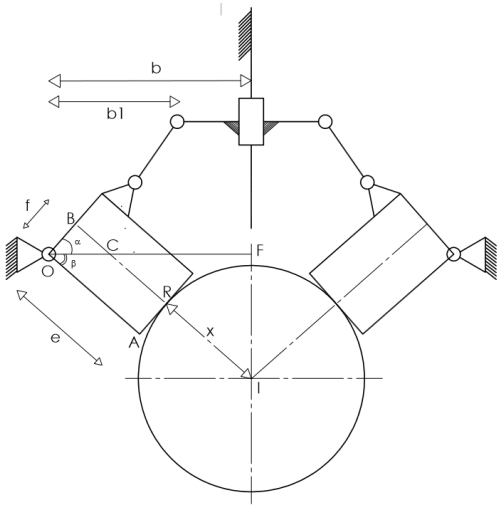

Fig. 6: Kinematics of the robot: $b = 72mm$, $b_1 = 45mm$, $f = 11mm$, and $e = 55mm$.

From Fig. 6: $x = IC - CR$, in which, $IC = \dfrac{CF}{\cos\beta} = \dfrac{OF - OC}{\cos\beta} = \dfrac{b - \dfrac{f}{\cos\alpha}}{\cos\beta} = \dfrac{b}{\cos\beta} - \dfrac{f}{\cos\alpha\cos\beta}$;

$CR = e - BC = e - f\tan\alpha$ with $\alpha + \beta = 90^{\circ}$;

$$\rightarrow x = \frac{b}{\cos\beta} - \frac{b}{\cos\alpha\cos\beta} - e + f\tan\alpha. \quad (3)$$

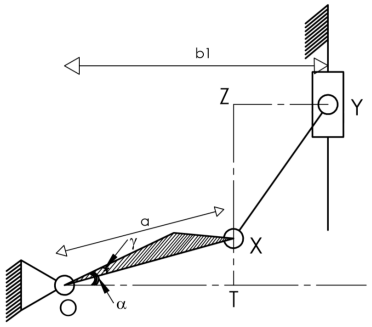

Fig. 7: Reciprocating mechanism: $a = 33.7mm$, $XY = 32mm$, and $\gamma = 12^\circ$

From Fig. 7: $y = XZ = \sqrt{XY^2 - YZ^2}$, where $YZ = b_1 - OT \Leftrightarrow YZ = b_1 - OX\cos\phi; (\phi = \alpha - \gamma)$;

$$\rightarrow y = \sqrt{XY^2 - (b_1 - a\cos\phi)^2}. \quad (4)$$

From equations (2), (3) and the designed gear ratio (1:19), we can calculate radius x of the steel cylinder based on rotations of the transformation motor. Robot is designed to work on steel cylinders having a smallest radius from $+5cm$ to $-25cm$ with $7.5cm$ feed screw movement.

B. Sliding Failure Investigation

To maintain stability of the robot while climbing on steel structures, the sliding and turn-over failures as illustrated in Fig. 8 (a,b) should be investigated.

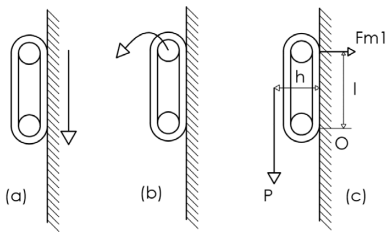

Fig. 8: a) Sliding failure; b) Turn-over failure; (c) Moment calculation at point O.

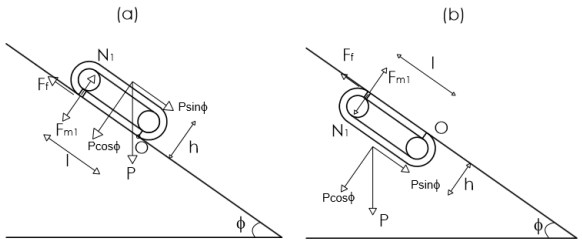

Fig. 9: a) Climbing on top inclined surface; b) Climbing underneath inclined surface.

In general case, based on the proposed design, the robot is able to climb on different shapes of structures (cylinder, cube or flat) with different inclination levels as shown in Fig. 9. In this analysis, we focus on basic working condition-flat surface to calculate the needed magnets and motor's parameters, then do experiments on different surfaces (curving, cube) in different conditions to find out optimal results.

Let P be the robot's total weight ($P = mg$, where m is the robot's mass, and g is the gravitational acceleration). Let F_m be the magnetic adhesion force, N be the reaction force, μ be the frictional coefficient, F_f be frictional force, and ϕ be the degree of inclination. Denote $\sum F$ as the total force applied to the robot. Based on Newton's second law of motion, $\sum F = 0$ when the robot stops.

When the robot climbs on top of an inclined surface (Fig. 9a), based on our previous work [25], we can obtain the magnetic adhesion force: $F_m = \dfrac{P\sin\phi}{\mu} - P\cos\phi$. Hence, the sliding failure can be avoided if the magnetic force satisfies the following condition:

$$F_m > \frac{P\sin\phi}{\mu} - P\cos\phi. \quad (5)$$

When the robot climbs underneath an inclined surface (Fig. 9b), we obtain: $F_m = \dfrac{P\sin\phi}{\mu} + P\cos\phi$. In this case, the magnetic force should be

$$F_m > \frac{P\sin\phi}{\mu} + P\cos\phi. \quad (6)$$

When the robot climbs on a vertical surface ($\phi = 90^o$)

$$F_m > \frac{P}{\mu}. \quad (7)$$

From inequations (5), (6) and (7), to avoid sliding failure in any cases, the magnetic force should be

$$F_m > max\Big\{\frac{P\sin\phi}{\mu} - P\cos\phi; \frac{P\sin\phi}{\mu} + P\cos\phi\Big\}. \quad (8)$$

Since $0 < \phi \leq 90 \Rightarrow \cos\phi \geq 0$, the overall condition for avoiding sliding failure should satisfy condition in inequation (6). Assume that the frictional coefficient μ between two roller-chains and steel surface is from $[0.4 - 0.8]$, we see that $\Big(\dfrac{\sin\phi}{\mu} + \cos\phi\Big)$ decreases when μ increases, or we have:

$$0.4 \leq \mu \leq 0.8; 0 < \phi \leq 90$$
$$\Rightarrow max\Big\{\frac{\sin\phi}{\mu} + \cos\phi\Big\} = 2.5 \Rightarrow F_m \geq 2.5P.$$

In summary, the robot's magnetic adhesion force should be greater or equal to 2.5 of the robot's weight.

C. Turn-over Failure Investigation

Let l be the distance between first and last magnet block contacting to the surface, and h be the distance between the center of mass to the surface (Fig. 8c). Moment at point O (the point that the first magnet block contacts the steel surface) is calculated as follows:

$$\sum M = P * h - 2F_{m_1} * l = 0 \Leftrightarrow F_{m_1} = \frac{P * h}{2l}.$$

To avoid turn-over failure, the magnetic force of the first contacting magnet block:

$$F_{m_1} > \frac{P * h}{2l}. \quad (9)$$

From (9), to avoid the turn-over failure we can lower $\dfrac{h}{l}$, which means making the robot's center of mass closer to the steel surface. In the proposed design (Fig. 5), $h = 4.6$cm, and the total robot height $h_r = h + 9.231cm = 19.751$cm.

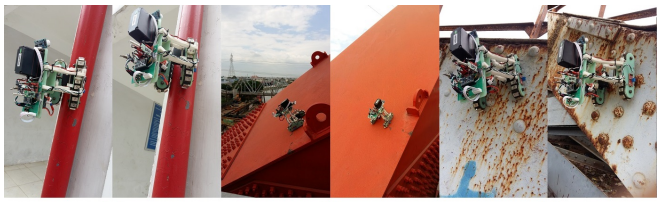

Fig. 10: Adhesion and climbing test on: (a) a thin paint-coated steel structure: cylinder shape D=100mm; (b) a thick paint-coated steel bridge: flat surface; (c) a rusty paint-coated steel bridge: flat structure with bolts/nuts.

Therefore, to avoid both sliding and turn-over failures, the robot's magnetic force of each magnet block should satisfy:

$$F_{m_j}(j = 1 : n) > max\Big\{\frac{2.5P}{n}; \frac{P * h_r}{2l}\Big\}. \quad (10)$$

Following the proposed design, $P = 30$N, $n = 16$ magnet blocks (each roller-chain has maximum 8 magnet blocks contacting the steel surface), $l = 9.8$cm, or $F_{m_j}(j = 1 : 16) > max\Big\{\frac{2.5 * 3}{16}; \frac{3 * 19.751}{2 * 9.8}\Big\} > 3(N)$.

IV. Robot Deployment

To evaluate design and performance of the robot, experiments for evaluating the magnetic force created by roller-chains have been conducted. The ability of climbing and failure avoidance were tested. During the test, a Lipo battery (2 cells) 7.4V 900 milliampere-hour (mAh) is used to power the robot for about 1 hour of working. One laptop, which can connect to a wireless LAN, is used as a ground station. The robot's mass $m = 3kg$, and if we assume that the gravitational acceleration $g = 10m/s^2$, the total weight of the robot is approximately $P = mg = 30N$. Since $15mm \times 10mm \times 5mm$ magnet blocks are used, the total magnetic force satisfies magnetic force condition as presented in equation (10).

TABLE III: Statistical result.

Structrural parameters	Decription
Thinnest steel surface	1 (mm)
Smallest steel cylinder diameter	100 (mm)
Thickest coated paint	4 (mm)
Highest nut or bolt area	12 (mm)

The outdoor experiments and robot deployments are conducted on several steel bridges. Some typical climbing examples are shown in Fig. 10. The steel structures have different thicknesses of paint coated on steel surfaces. Some paint-coated steel surfaces are very rusty, some are not clean, and some others are still in fine condition (minor-rusty). Statistical results with description of specifications that the robot can work with is presented in Tab. III.

During the experiments, the climbing capability tests are done on steel bridges and steel structures, and on with coated or unclean surfaces as seen on Fig. 10. The robot is able to adhere very well on these steel structures while climbing with maximum speed is 200 mm/s during 1 hour. Even for the case of curving surface (Fig. 10a), the robot can still adhere tightly to the steel structures while performing the climb. For rusty steel surfaces, it also shows strong climbing capability

Fig. 11: Images stitching result: (Top) 7 individual images taken by the robot climbing on a bridge in Fig. 10; (Middle) Stitching image result from those 7 individual images; (Bottom) Closer look (zoom-in) at some areas, which has serious rusty condition with holes on the surface.

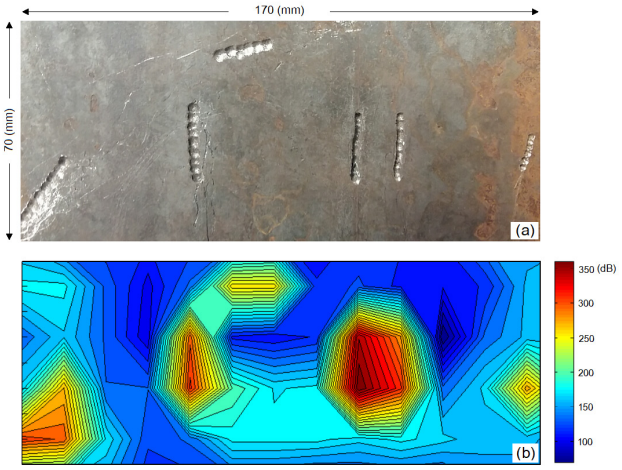

Fig. 12: (a) Image of an inspected area with cracks on it; (b) Fatigue crack map from Eddy current sensor showing defect areas with red/yellow color, corresponding well with the crack areas on the image.

(Fig. 10c). However, in some very tough conditions, such as bird drops or high nuts, the robot might loose adhesion force and can not pass these areas. Robot deployments can be seen in the youtube link: `https://www.youtube.com/watch?time_continue=41&v=1Wl9Trd3EoM`

The robot is controlled to move and stop at every certain distance (e.g., 12cm) to capture images of steel surfaces and do closer investigation on potential crack areas, then send collected data to the ground station. To enhance steel surface inspection, acquired images are then stitched together to produce an overall picture of a steel surface as shown in Fig. 11. The image stitching is followed by our previously developed algorithm [32].

In addition to the visual data collection, the robot also collects Eddy current data. The survey is conducted on a $170 \times 70mm$ area, which contains some crack areas as shown in Fig. 12a. The robotic arm holds the Eddy current sensor's probe and performs a zig-zag path consisting of four lines. For the ease of illustration, a color coded map is built as shown in Fig. 12b, and we can see that the Eddy current condition/fatigue crack map has defect areas (red/yellow color) correlating very well with the crack areas on the image.

V. Conclusion and Future Work

This paper presents a new development of a tank-like robot, which is capable of climbing on different steel structure shapes to perform inspection. The robot design is implemented and validated on climbing on more than 20 different steel bridges. During the tests, the robot is able to firmly adhere on steel structures with various inclination levels. Rigorous analysis of magnetic adhesion force has been performed to confirm that the robot is able to adhere to both flat and curving steel surfaces in various conditions (coated, non-coated and/or rusty.) Various experiments have been conducted including magnetic force measurement, indoor and outdoor climbing tests in order to validate the force analysis as well as the climbing capability of the robot. The results show that when the magnetic adhesion force requirement is met, the robot is able to move and transition safely between steel surfaces without any failures. Multiple sensors are integrated to assist the robot's navigation as well as data collection. The rigorous magnetic force analysis can serve as a framework to calculate and design different types of steel inspection robots in the future. Inspection data (Eddy current and visual) is collected and transferred to ground station for visualization and processing.

Further works can be focusing localization using odometry, IMU and visual data, and implementation of map construction methods as well as visual crack detection algorithms. Besides, the robot can be further improved to move in circumferential directions on small diameter cylinder-like objects.

References

[1] U.S Department of transportation highway administration, national bridge inventory data. http://www.fhwa.dot.gov/bridge/nbi.cfm.

[2] H. M. La, N. Gucunski, K. Dana, and S.-H. Kee. Development of an autonomous bridge deck inspection robotic system. *Journal of Field Robotics*, 34(8):1489–1504, 2017.

[3] Crews inspect condition of golden gate bridge's towers, April 30, 2018. https://www.nbcbayarea.com/on-air/as-seen-on/Crews-Inspect-Condition-of-Golden-Gate-Bridge_s-Towers_Bay-Area-481315951.html.

[4] W. Fischer, F. Tâche, and R. Siegwart. *Magnetic Wall Climbing Robot for Thin Surfaces with Specific Obstacles*, pages 551–561. Springer Berlin Heidelberg, Berlin, Heidelberg, 2008.

[5] W. Fischer, G. Caprari, R. Siegwart, and R. Moser. Locomotion system for a mobile robot on magnetic wheels with both axial and circumferential mobility and with only an 8-mm height for generator inspection with the rotor still installed. *IEEE Transactions on Industrial Electronics*, 58(12):5296–5303, Dec 2011.

[6] P. Ratsamee, P. Kriengkomol, T. Arai, K. Kamiyama, Y. Mae, K. Kiyokawa, T. Mashita, Y. Uranishi, and H. Takemura. A hybrid flying and walking robot for steel bridge inspection. In *IEEE Inter. Symp. on Safety, Security, and Res. Robo.*, pages 62–67, Oct 2016.

[7] H. M. La, T. H. Dinh, N. H. Pham, Q. P. Ha, and A. Q. Pham. Automated robotic monitoring and inspection of steel structures and bridges. *Robotica*, pages 1 – 21, 2018.

[8] W. Shen, J. Gu, and Y. Shen. Permanent magnetic system design for the wall-climbing robot. In *IEEE Intern. Conf. Mechatronics and Automation, 2005*, volume 4, pages 2078–2083 Vol. 4, July 2005.

[9] A. Mazumdar and H. H. Asada. Mag-foot: A steel bridge inspection robot. In *Intelligent Robots and Systems, 2009. IROS 2009. IEEE/RSJ Intern. Conf. on*, pages 1691–1696, Oct 2009.

[10] R. Wang and Y. Kawamura. A magnetic climbing robot for steel bridge inspection. In *Intelligent Control and Automation (WCICA), 2014 11th World Congress on*, pages 3303–3308, June 2014.

[11] F. Tche, W. Fischer, G. Caprari, R. Siegwart, R. Moser, and F. Mondada. Magnebike: A magnetic wheeled robot with high mobility for inspecting complex-shaped structures. *Journal of Field Robotics*, 26(5):453–476, 2009.

[12] A. Leibbrandt, G. Caprari, U. Angst, R. Y. Siegwart, R.J. Flatt, and B. Elsener. Climbing robot for corrosion monitoring of reinforced concrete structures. In *Applied Robotics for the Power Industry (CARPI), the 2nd Intern. Conf. on*, pages 10–15, Sept 2012.

[13] H. Leon-Rodriguez, S. Hussain, and T. Sattar. A compact wall-climbing and surface adaptation robot for non-destructive testing. In *Control, Automation and Systems (ICCAS), 2012 12th Intern. Conf. on*, pages 404–409, Oct 2012.

[14] A. San-Millan. Design of a teleoperated wall climbing robot for oil tank inspection. In *Control and Automation (MED), 2015 23th Mediterranean Conference on*, pages 255–261, June 2015.

[15] W. Shen, J. Gu, and Y. Shen. Proposed wall climbing robot with permanent magnetic tracks for inspecting oil tanks. In *IEEE Intern. Conf. Mechatronics and Automation, 2005*, volume 4, pages 2072–2077 Vol. 4, July 2005.

[16] M. Tavakoli, C. Viegas, L. Marques, J. N. Pires, and A. T. de Almeida. Omniclimbers: Omni-directional magnetic wheeled climbing robots for inspection of ferromagnetic structures. *Robotics and Autonomous Systems*, 61(9):997 – 1007, 2013.

[17] M. Eich and T. Vgele. Design and control of a lightweight magnetic climbing robot for vessel inspection. In *the 19th Mediterranean Conf. on Control Automation*, pages 1200–1205, June 2011.

[18] D. Zhu, J. Guo, C. Cho, Y. Wang, and K. Lee. Wireless mobile sensor network for the system identification of a space frame bridge. *IEEE/ASME Trans. on Mechatronics*, 17(3):499–507, June 2012.

[19] G. Lee, G. Wu, J. Kim, and T. Seo. High-payload climbing and transitioning by compliant locomotion with magnetic adhesion. *Robotics and Autonomous Systems*, 60(10):1308 – 1316, 2012.

[20] T. Seo and M. Sitti. Tank-like module-based climbing robot using passive compliant joints. *IEEE/ASME Transactions on Mechatronics*, 18(1):397–408, Feb 2013.

[21] R. Wang and Y. Kawamura. A magnetic climbing robot for steel bridge inspection. In *Proceeding of the 11th World Congress on Intelligent Control and Automation*, pages 3303–3308, June 2014.

[22] J. Guo, W. Liu, and K. M. Lee. Design of flexonic mobile node using 3d compliant beam for smooth manipulation and structural obstacle avoidance. In *2014 IEEE Intern. Conf. on Robotics and Automation (ICRA)*, pages 5127–5132, May 2014.

[23] S. Kamdar. Design and manufacturing of a mecanum sheel for the magnetic climbing robot. *Master Thesis, Embry-Riddle Aeronautical University*, May 2015.

[24] P. Ward, P. Manamperi, P. R. Brooks, P. Mann, W. Kaluarachchi, L. Matkovic, G. Paul, C. H. Yang, P. Quin, D. Pagano, D. Liu, K. Waldron, and G. Dissanayake. Climbing robot for steel bridge inspection: Design challenges. In *Austroads Publications Online, ARRB Group*, 2015.

[25] N. H. Pham and H. M. La. Design and implementation of an autonomous robot for steel bridge inspection. In *54th Allerton Conf. on Comm., Con., and Comp.*, pages 556–562, Sept 2016.

[26] R. Wang and Y. Kawamura. Development of climbing robot for steel bridge inspection. *Industrial Robot: An International Journal*, 43(4):429–447, 2016.

[27] N. H. Pham, H. M. La, Q. P. Ha, S. N. Dang, A. H. Vo, and Q. H. Dinh. Visual and 3d mapping for steel bridge inspection using a climbing robot. In *The 33rd Intern. Symposium on Automation and Robotics in Construction and Mining (ISARC)*, pages 1–8, July 2016.

[28] Y. Takada, S. Ito, and N. Imajo. Development of a bridge inspection robot capable of traveling on splicing parts. *Inventions*, 2, 2017.

[29] Versatrax 150^{TM}. http://inuktun.com/en/products/.

[30] H. M. La, R. S. Lim, B. B. Basily, N. Gucunski, J. Yi, A. Maher, F. A. Romero, and H. Parvardeh. Mechatronic systems design for an autonomous robotic system for high-efficiency bridge deck inspection and evaluation. *IEEE/ASME Transactions on Mechatronics*, 18(6):1655–1664, Dec 2013.

[31] H. M. La, N. Gucunski, Seong-Hoon Kee, J. Yi, T. Senlet, and Luan Nguyen. Autonomous robotic system for bridge deck data collection and analysis. In *2014 IEEE/RSJ Intern. Conf. on Intelligent Robots and Systems*, pages 1950–1955, Sep. 2014.

[32] H. M. La, N. Gucunski, S.-H. Kee, and L.V. Nguyen. Data analysis and visualization for the bridge deck inspection and evaluation robotic system. *Visualization in Engineering*, 3(1):1–16, 2015.